

Chapter 5

Shadowing Corrections to the Small- x Behaviour of Gluon Distribution Function

5.1 Introduction

The dynamics of the the high density QCD, the regime of large gluon densities, is one of the present-day extremely demanding undecided issues in the area of high energy or small- x physics, where x is the small fraction of proton's momentum conveyed by the struck parton. Enormous theoretical and experimental endeavours towards the perception of hadron structure in the high density regime at small- x occurs from DIS at HERA to the proton-(anti)proton collisions at LHC. The gluon saturation is one of the most fascinating problems of the small- x physics, which is presumed on theoretical basis and there is emerging indications of its existence [1-3]. The linear QCD evolution equations at the twist-2 level like DGLAP [4-6] predicts an abrupt rise of the gluon densities towards small- x which is also perceived in the DIS experiments at HERA. This sharp growth of gluon density generates cross sections which in the high-energy limit violate the Froissart bound [7, 8] on physical cross sections. Accordingly a new formulation of the QCD at high partonic density is essential, in the very small- x region, to incorporate the unitarity corrections in a suitable way. In general it is anticipated that, the gluon recombination processes provide the mechanism responsible for the unitarization of the cross section at high energies. As we move towards small- x at fixed Q^2 the number of gluons of fixed size

$\sim 1/Q$ increases and at some critical value of x , the entire transverse area inhabited by gluons turns out to be analogous to or larger than the transverse area of a proton. Thus, the likelihood of interaction between two gluons can no longer be overlooked and it sooner or later engenders a situation in which individual partons inevitably overlap or shadow each other. In the derivation of the linear DGLAP equation the correlations among the initial gluons in the physical process of interaction and recombination of gluons are not usually taken into account. But at small- x the corrections of the correlations among the initial gluons to the evolutionary amplitude should be considered which eventually leads to a control of the maximum gluon density per unit of phase-space. The conventional linear DGLAP evolution equation will have to be modified accordingly in order to take these into effect. The multiple gluon interactions take part in the evolution nonlinearly, taming the growth of the gluon density in the kinematic domain where α_s remains small but the density of gluons evolves into very high. The pioneering perturbative QCD studies reporting the recombination of two gluon ladders into one were performed by Gribov, Levin and Ryskin [9], and by Mueller and Qiu [10, 11]. They insinuated that the shadowing or nonlinear corrections due to gluon recombination could be expressed in a new evolution equation with an additional nonlinear term quadratic in gluon density. This equation, widely known as the GLR-MQ equation, can be regarded as the upgraded version of the linear DGLAP equation.

The GLR-MQ equation incorporates all fan diagrams, that is, all workable $2 \rightarrow 1$ ladder recombinations, in the double leading logarithmic approximation (DLLA) in order to deal with the gluon recombination processes. The fan diagrams portrays the decisive role in the restoration of unitarity by taking into consideration some of the gluon recombination processes that become vital at small- x . Gribov, Levin and Ryskin at the outset introduced the concept of shadowing, arising from gluon recombination, based on the Abramovsky-Gribov-Kancheli (AGK) cutting rule [12] in the DLLA. Later Mueller and Qiu successfully carried out a perturbative calculation of the recombination probabilities in the DLLA which empowers the equation to be applied phenomenologically [10]. The GLR-MQ equation prognosticate a critical line separating the perturbative regime from the saturation regime and it is legitimate only in the vicinity of this critical line. Moreover it predicts a saturation of the gluon

density at very small- x . Therefore the study of the GLR-MQ equation is extremely important for understanding the nonlinear effects of gluon recombination at small enough x as well as for the determination of the saturation momentum (Q_S) that incorporates physics in addition to that of the linear evolution equations commonly used to fit DIS data.

Until now the majority of our knowledge on the modifications of the higher order QCD effects is established on the semi-classical approach [9, 13-15] and on numerical studies [16-21]. The approximate analytical solutions of the nonlinear GLR-MQ evolution equation have also been reported in recent years [22, 23]. In this thesis we attempt to use, to a feasible extent, semi-analytic methods to solve this equation. We report, in this chapter, the approximate semi-analytical solution of the nonlinear GLR-MQ equation as well as the validity of the well known Regge-like ansatz in the region of small- x and moderate virtuality of photon. The aim of this work is to check the evidence for gluon recombination at very small- x . We investigate the effect of shadowing corrections on the small- x behavior of gluon distribution at fixed virtuality of photon from the solution of GLR-MQ equation in LO with considerable phenomenological success. Moreover, we obtain the Q^2 -dependence of gluon distribution with shadowing corrections at fixed small- x . Our resulting gluon distributions are compared with different experimental data and parametrizations. Our predictions for nonlinear gluon density are further compared with different models based on GLR-MQ equation. Moreover, we examine the extent of nonlinearity in our predictions by comparing the gluon distributions obtained from nonlinear GLR-MQ equation with those obtained from linear DGLAP equation.

5.2 Formalism

5.2.1 General framework

The GLR-MQ equation depends on two processes in the parton cascade, namely the gluon emission generated by the QCD vertex $g \rightarrow g + g$ as well as the gluon recombination by the same vertex $g + g \rightarrow g$. The probability that a gluon splits into two gluons is proportional to $\alpha_s \rho$ whereas the probability of gluon recombination is proportional to $\alpha_s^2 r^2 \rho^2$. Here, ρ is the density of gluons in the transverse plane and r is the size of the gluon produced in the recombination process and for DIS, $r \propto \frac{1}{Q}$.

It is very clear that, at $x \sim 1$ only the production of new partons (quarks or gluons) is essential because $\rho \ll 1$, however at $x \rightarrow 0$ the value of ρ becomes so large that the recombination of gluons turns into crucial. The number of partons in a phase space cell ($\Delta \ln(1/x) \Delta \ln Q^2$), thus, increases through gluon splitting and decreases through gluon recombination and correspondingly the balance equation for emission and recombination of partons can be written as [9-11]

$$\frac{\partial^2 \rho(x, Q^2)}{\partial \ln(1/x) \partial \ln Q^2} = \frac{\alpha_s(Q^2) N_c}{\pi} \rho(x, Q^2) - \frac{\alpha_s^2(Q^2) \gamma}{Q^2} [\rho(x, Q^2)]^2, \quad (5.1)$$

which is referred to as the GLR-MQ equation. Here $\rho = \frac{xg(x, Q^2)}{\pi R^2}$, where πR^2 is the target area and R is the correlation radius between two interacting gluons i.e. the size of the relevant region for the gluon recombination processes. The factor γ is found to be $\gamma = \frac{81}{16}$ for $N_c = 3$, as evaluated by Mueller and Qiu [10]. In terms of gluon distribution function the above equation can be expressed as

$$\frac{\partial^2 xg(x, Q^2)}{\partial \ln(1/x) \partial \ln Q^2} = \frac{\alpha_s(Q^2) N_c}{\pi} xg(x, Q^2) - \frac{\alpha_s^2(Q^2) \gamma}{\pi Q^2 R^2} [xg(x, Q^2)]^2, \quad (5.2)$$

The first term in the r.h.s. is the usual DGLAP term in the DLLA and is therefore linear in the gluon field. The second term carries a negative sign and it reduces the growth of the gluon distribution once the fan diagrams become admissible. It expresses the nonlinearity in respect of the square of the gluon distribution. Here, the representation for the gluon distribution $G(x, Q^2) = xg(x, Q^2)$ is used, where $g(x, Q^2)$ is the gluon density. The quark-gluon emission diagrams are not given attention here due to their little importance in the gluon-rich small- x region. A general criterion for the validity of Eq.(5.2) is that the nonlinear correction term should not be larger than the first term since in that case further corrections must be considered and non-perturbative effects could be of importance [24].

The parameter R does not become operative as long as one uses the DGLAP evolution equation, which is linear in gluon density. Nonetheless, this size parameter becomes relevant in the GLR-MQ equation where one takes into account the first nonlinear term in the evolution and therefore it is essential to define it precisely. Since the size parameter R in the denominator and the gluon distribution G in the numerator appear in the second term of Eq.(5.2) as squared, so they are extremely decisive for the magnitude of the recombination effect. R is of the order of proton

radius R_h , that is $R \sim 5 \text{ GeV}^{-1}$ if the gluons are distributed uniformly across the whole of the proton and in that case recombination or shadowing corrections can be negligibly small [10, 25]. On the other hand, R is of the order of the transverse size of a valence quark i.e. $R \sim 2 \text{ GeV}^{-1}$ if the gluons are condensed in the hot spots [10, 25, 26] inside the proton. The hot spots can enumerate rapid commencement of gluon-gluon interactions in the environs of the parton and and so uplift the recombination effect. Accordingly in such hot-spots the shadowing corrections are expected to be large.

5.2.2 Solution of GLR-MQ equation for gluon distribution function and effect of gluon shadowing

In order to study the effect of nonlinear or shadowing corrections on the behaviour of gluon density we rewrite the GLR-MQ equation given by Eq.(5.2) in a convenient form

$$\frac{\partial G(x, Q^2)}{\partial \ln Q^2} = \frac{\partial G(x, Q^2)}{\partial \ln Q^2} \Big|_{DGLAP} - \frac{81}{16} \frac{\alpha_s^2(Q^2)}{R^2 Q^2} \int_x^1 \frac{d\omega}{\omega} \left[G\left(\frac{x}{\omega}, Q^2\right) \right]^2, \quad (5.3)$$

We perform the analysis in the leading twist approximation and therefore have taken the strong coupling constant $\alpha_s(Q^2) = \frac{4\pi}{\beta_0 \ln(Q^2/\Lambda^2)}$, where $\beta_0 = 11 - \frac{2}{3}N_f$. At small- x gluons essentially turn out to be the most abundant partons and therefore, the quark contributions to the gluon distribution function can be overlooked in the small- x region. Accordingly the first term in the r.h.s. of Eq. (5.3) can be expressed as [27]

$$\begin{aligned} \frac{\partial G(x, Q^2)}{\partial \ln Q^2} \Big|_{DGLAP} = & \frac{3\alpha_s(Q^2)}{\pi} \left[\left(\frac{11}{12} - \frac{N_f}{18} + \ln(1-x) \right) G(x, Q^2) \right. \\ & + \int_x^1 d\omega \left\{ \frac{\omega G\left(\frac{x}{\omega}, Q^2\right) - G(x, Q^2)}{1-\omega} \right. \\ & \left. \left. + \left(\omega(1-\omega) + \frac{1-\omega}{\omega} \right) G\left(\frac{x}{\omega}, Q^2\right) \right\} \right]. \quad (5.4) \end{aligned}$$

To obtain an analytical solution of the GLR-MQ equation in the small- x region we incorporate a Regge-like behavior of gluon distribution function. The behaviour of structure functions at small- x can be described effectively in terms of Regge-like ansatz [28]. The Regge theory is a highly ingenious parameterization of all total cross sections and supposed to be applicable at large- Q^2 values if x is small enough $x < 0.01$ [29]. Moreover, as advocated in Refs.[30, 31], the Regge behavior is anticipated to

be valid at small- x and some intermediate Q^2 , where Q^2 must be small but not so small that $\alpha_s(Q^2)$ is too large. Since the total center of mass energy squared is defined as $s^2 = Q^2(\frac{1}{x} - 1)$, therefore the small- x behaviour of structure functions for fixed Q^2 emulates the high energy behaviour of total cross section with increasing s^2 [32]. For this reason the Regge pole exchange picture [28] sounds convenient for the theoretical description of this behaviour. Again, as the structure functions are proportional to the total virtual photon-nucleon cross section, therefore they are expected to have Regge behaviour corresponding to pomeron or reggeon exchange [30]. According to the Donnachie-Landshoff (DL) model, the high energy attitude of hadronic cross sections as well as structure functions will be governed by two contributions, especially by a pomeron proliferating the rise of structure function at small- x and by reggeons related with meson trajectories. The high energy i.e. small- x behaviour of both gluons and sea quarks are conducted by the same singularity factor in the complex angular momentum plane [31] in accordance with Regge theory. The Regge behavior of the sea-quark distribution for small- x is given by $q_{sea}(x) \sim x^{-\alpha_P}$ corresponding to a pomeron exchange with an intercept of $\alpha_P = 1$. But the valence-quark distribution for small x given by $q_{val}(x) \sim x^{-\alpha_R}$ corresponds to a reggeon exchange with an intercept of $\alpha_R = 0.5$. The x dependence of the parton densities is often estimated at moderate Q^2 and thus the leading order calculations in $\ln(1/x)$ with fixed α_s predict a steep power-law behavior of $xg(x, Q^2) \sim x^{-\lambda_G}$, where $\lambda_G = (4\alpha_s N_c/\pi) \ln 2 \simeq 0.5$ for $\alpha_s \simeq 0.2$, as relevant for $Q^2 \sim 4 \text{ GeV}^2$.

Furthermore, the Regge theory is presumed to be applicable if W^2 , the mass invariant squared in a DIS process, is much greater than all the other variables [33] and so, models based upon this idea have been fruitful in explaining the DIS cross-section when x is small enough ($x < 0.7$), whatsoever be the value of Q^2 [33-35]. The small- x limit of DIS corresponds to the case when $2M\nu \gg Q^2$, where $x = Q^2/2M\nu$, but Q^2 is still maintained large i.e. $Q^2 > \Lambda^2$, with Λ being the QCD cut off parameter. The limit $2M\nu \gg Q^2$ is equivalent to $s \gg Q^2$ and is therefore the Regge limit of DIS. Moreover, as Q remains greater than the QCD cut off parameter Λ so it enables us to use perturbative QCD calculations and therefore Regge theory is applicable in the region of large s , i.e. in the region of small- x [28, 29]. Hence it is feasible to use Regge theory for the study of the GLR-MQ equation which is an improved version

of DGLAP equation in the very small- x region. The Regge pole model gives the parametrization of the DIS structure function $F_2(x, Q^2)$ at small- x as $F_2 \propto x^{-\lambda}$ with $\lambda > 0$ being a constant or depending on Q^2 or x [29, 33].

On that account, we employ the Regge like ansatz of gluon distribution function to solve the nonlinear GLR-MQ equation at small- x . We assume a simple form of Regge ansatz for gluon distribution function given as

$$G(x, Q^2) = H(Q^2)x^{-\lambda_G}, \quad (5.5)$$

where $H(Q^2)$ is a function of Q^2 and λ_G is the Regge intercept for gluon distribution function. This form of Regge behaviour is extensively used by many authors with considerable success [33, 36, 37]. With this ansatz the term $G(\frac{x}{\omega}, Q^2)$ can be written as

$$G\left(\frac{x}{\omega}, Q^2\right) = \omega^{\lambda_G} G(x, Q^2). \quad (5.6)$$

One of the applications of the Regge behaviour is the DL two pomeron model where the rise of structure function is described by powers of $1/x$. In the DL model it is assumed that the exchange of two pomerons contribute to the amplitude, however, at small- x the gluon distribution function is dominated exclusively by the hard pomeron exchange [33]. In the DL two pomerons exchange model, the hard pomeron has an intercept $\epsilon_h = 0.418$. Moreover, as the values of Regge intercepts for all the spin-independent singlet, non-singlet and gluon structure functions should be close to 0.5 in quite a broad range of small- x [37], so we also consider the value of λ_G to be 0.5 in our analysis and expect to obtain our best fit results with this value of λ_G .

To simplify our calculations we consider a variable t , such that $t = \ln(\frac{Q^2}{\Lambda^2})$. Then using the Eqs.(5.5) and (5.6) together with the Eq.(5.4), Eq.(5.3) can be simplified as

$$\begin{aligned} \frac{\partial G(x, t)}{\partial t} &= \frac{3\alpha_s(t)}{\pi} G(x, t) \left[\left(\frac{11}{12} - \frac{N_f}{18} + \ln(1-x) \right) + \int_x^1 d\omega \left\{ \frac{\omega^{\lambda_G+1} - 1}{1-\omega} \right. \right. \\ &\quad \left. \left. + \left(\omega(1-\omega) + \frac{1-\omega}{\omega} \right) \omega^{\lambda_G} \right\} \right] - \frac{81}{16} \frac{\alpha_s^2(t)}{R^2 \Lambda^2 e^t} G^2(x, t) \int_x^1 \omega^{2\lambda_G-1} d\omega. \end{aligned} \quad (5.7)$$

Now rearranging the terms Eq. (5.7) can be expressed as

$$\frac{\partial G(x, t)}{\partial t} = \gamma_1(x) \frac{G(x, t)}{t} - \gamma_2(x) \frac{G^2(x, t)}{t^2 e^t}, \quad (5.8)$$

where the x dependent functions $\gamma_1(x)$ and $\gamma_2(x)$ are defined as

$$\gamma_1(x) = 3A_f \left[\frac{11}{12} - \frac{N_f}{18} + \ln(1-x) + \int_x^1 d\omega \left\{ \frac{\omega^{\lambda_G+1} - 1}{1-\omega} + \left(\omega(1-\omega) + \frac{1-\omega}{\omega} \right) \omega^{\lambda_G} \right\} \right], \quad (5.9)$$

$$\gamma_2(x) = \frac{81}{16} \frac{A_f^2 \pi^2}{R^2} \int_x^1 \omega^{2\lambda_G-1} d\omega. \quad (5.10)$$

where $A_f = \frac{4}{\beta_0}$.

Eq.(5.8) is a partial differential equation for the gluon distribution function with respect to the variables x and Q^2 ($t = \ln(Q^2/\Lambda^2)$). Thus apart from its conventional use in Q^2 -evolution, Eq.(5.8) can also be used to examine the x -dependence of gluon distribution. Solution of Eq.(5.8) then leads us to a solution for the nonlinear gluon density as given below

$$G(x, t) = \frac{t^{\gamma_1(x)}}{C + \gamma_2(x) \int t^{\gamma_1(x)-2} e^{-t} dt}, \quad (5.11)$$

where C is a constant to be determined from initial boundary conditions. Thus we solve Eq.(5.3) by employing the Regge ansatz for gluon distribution given by Eq.(5.5) and obtain a solution of the nonlinear gluon density. As the Regge behaviour is supposed to be legitimate at small- x and some intermediate Q^2 , therefore the solution of the GLR-MQ equation in the form of Eq.(5.11) is expected to be worthwhile. We believe that our solution is correct in the vicinity of the saturation where all our assumptions look natural. Now to determine the Q^2 ($t = \ln(Q^2/\Lambda^2)$) and x -dependence of the gluon distribution we apply the following two physically plausible boundary conditions

$$G(x, t) = G(x, t_0) \quad (5.12)$$

at some lower value $Q^2 = Q_0^2$, where $t_0 = \ln(Q_0^2/\Lambda^2)$ and

$$G(x, t) = G(x_0, t), \quad (5.13)$$

at some high $x = x_0$.

The boundary condition (5.12) gives us

$$G(x, t_0) = \frac{t_0^{\gamma_1(x)}}{C + \gamma_2(x) \int t_0^{\gamma_1(x)-2} e^{-t_0} dt_0}, \quad (5.14)$$

From this equation the constant C can be evaluated by considering an appropriate input distribution $G(x, t_0)$ at a given value of Q_0^2 . Now Eq.(5.11) and Eq.(5.14) lead us to the Q^2 -evolution of gluon distribution function for fixed x given as

$$G(x, t) = \frac{t^{\gamma_1(x)} G(x, t_0)}{t_0^{\gamma_1(x)} + \gamma_2(x) \left[\int t^{\gamma_1(x)-2} e^{-t} dt - \int t_0^{\gamma_1(x)-2} e^{-t_0} dt_0 \right]} G(x, t_0). \quad (5.15)$$

Thus we have obtained an expression for the Q^2 -evolution of nonlinear gluon density at LO by solving the nonlinear GLR-MQ evolution equation semi-analytically. From this expression we can easily compute the dependence of gluon distribution function on Q^2 for a particular value of x by choosing an appropriate input distribution at a given value of Q_0^2 . Eq.(5.15) also assist us to investigate the nonlinear or shadowing corrections to the gluon distribution functions at moderate values of Q^2 .

Similarly, the boundary condition (5.13) yields

$$G(x_0, t) = \frac{t^{\gamma_1(x_0)}}{C + \gamma_2(x_0) \int t^{\gamma_1(x_0)-2} e^{-t} dt}, \quad (5.16)$$

so that using Eqs. (5.11) and (5.16) we obtain

$$G(x, t) = \frac{t^{\gamma_1(x)} G(x_0, t)}{t^{\gamma_1(x_0)} + \left[\gamma_2(x) \int t^{\gamma_1(x)-2} e^{-t} dt - \gamma_2(x_0) \int t^{\gamma_1(x_0)-2} e^{-t} dt \right]} G(x_0, t). \quad (5.17)$$

Thus Eq. (5.17) provides the solution of the GLR-MQ equation for gluon distribution at small- x for fixed Q^2 . Accordingly from Eq. (5.17) we can easily predict the small- x dependence of nonlinear gluon distribution function for a particular value of Q^2 by picking out a suitable input distribution at an initial value of $x = x_0$. The effect of nonlinear or shadowing corrections to the gluon distribution functions at small- x can be studied as well by employing Eq. (5.17).

We analyze the region of validity of our solution given by Eq.(5.11) and we expect that the solution is only valid in the region of small- x and intermediate values of Q^2 . It is clear from Eq.(5.11) that at large Q^2 ($t = \ln(Q^2/\Lambda^2)$), we can neglect the nonlinear corrections and our solution takes the form

$$G(x, t) = \frac{t^{\gamma_1(x)}}{C + \gamma_2(x) \int t^{\gamma_1(x)-2} e^{-t} dt} \xrightarrow{t \gg 1} t^{\gamma_1(x)} / C, \quad (5.18)$$

However, in the region where Q^2 is not very large, the corrections for the nonlinear term in Eq.(5.11) can not be neglected and in that case Eq.(5.11) does not reduce to Eq.(5.18). In our analysis we consider intermediate values of Q^2 ($1 \leq Q^2 \leq 30$

GeV²) to calculate the gluon distribution function. In this region the corrections for the nonlinear term $\gamma_2(x) \int t^{\gamma_1(x)-2} e^{-t} dt$ cannot be neglected in comparison to C , where C is defined by Eq.(5.14), and so our solution given by Eq.(5.11) does not reduce to Eq.(5.18).

On the other hand we observe that in the region $10^{-5} \leq x \leq 10^{-2}$ Eq.(5.11) predicts an increase of gluon distribution with decreasing- x , which is in accordance with the Regge ansatz of Eq.(5.5). Nevertheless Eq.(5.11) yields a slower growth of gluon density towards small- x in comparison to the solution of linear DGLAP equation, since the nonlinear effects due to gluon-gluon interactions play a significant role in the small- x ($x \leq 10^{-2}$) region. However in the region of very small- x ($x < 10^{-5}$) but fixed Q^2 , we can neglect the dependence of the functions $\gamma_1(x)$ and $\gamma_2(x)$ on x . Accordingly the solution suggested in Eq.(5.11) does not depend on x taking the form

$$G_{x \rightarrow 0}(x, t) = \frac{t^{\gamma_{10}}}{C + \gamma_{20} \int t^{\gamma_{10}} e^{-t} dt}, \quad (5.19)$$

where the r.h.s is a constant. In that case the solution to the nonlinear equation given by Eq.(5.11) contradicts the ansatz of Eq.(5.5). So we can conclude that Eq.(5.11) is not a valid solution at very small- x ($x < 10^{-5}$). It is to note that in the region of $x > 10^{-2}$ the process of gluon-recombination does not play an important role on the QCD evolution and therefore nonlinear corrections to the DGLAP equation is not essential. In other words in the region of $x > 10^{-2}$ DGLAP equation is sufficient to explain the available experimental data. So we can interpret that the solution given by Eq.(5.11) may not be applicable in the region of $x < 10^{-5}$ as well as $x > 10^{-2}$. But in the kinematic region $10^{-5} \leq x \leq 10^{-2}$ the x -dependence of the functions $\gamma_1(x)$ and $\gamma_2(x)$ can not be neglected and under this situation Eq.(5.11) does not reduce to Eq.(5.19) and thus it does not contradict the ansatz given by Eq.(5.5). Hence we can conclude that the solution suggested in Eq.(5.11) is expected to be a valid solution of the nonlinear GLR-MQ equation in the kinematic region $1 \leq Q^2 \leq 30$ GeV² and $10^{-5} \leq x \leq 10^{-2}$ and it can delineate the small- x dependence of nonlinear gluon density in a satisfactory manner.

5.2.3 Comparative analysis of DGLAP and GLRMQ equations

To estimate the effect of shadowing corrections for the gluon distribution function in our predictions we make a comparative study of the nonlinear GLR-MQ equation with the linear DGLAP approach. For this purpose we solve the linear DGLAP equation at small- x at LO defined by Eq.(5.4) by employing the Regge ansatz of gluon distribution function and compare it with the solution of the GLR-MQ equation discussed above. Using the Regge ansatz of Eq.(5.5), Eq.(5.4) can be simplified as

$$\left. \frac{\partial G(x, t)}{\partial t} \right|_{DGLAP} = \gamma_1(x) \frac{G(x, t)}{t}, \quad (5.20)$$

which can be easily solved to have

$$G(x, t) = At^{\gamma_1(x)}. \quad (5.21)$$

Here A is a constant to be fixed by initial boundary conditions. The x dependent function $\gamma_1(x)$ is defined in Eq.(5.9). Now defining

$$g_{10} = G(x, t_0) = At_0^{\gamma_1(x)} \quad (5.22)$$

at some lower value $Q^2 = Q_0^2$, we get from Eq.(5.21)

$$G(x, t) = g_{10} \left(\frac{t}{t_0} \right)^{\gamma_1(x)}. \quad (5.23)$$

Eq.(5.23) provides the solution of the linear DGLAP equation at LO for gluon distribution with the ansatz of Eq.(5.5) and it describes the Q^2 dependence of linear gluon density for a fixed value of x , provided a suitable input distribution g_{10} has been chosen from the initial boundary condition.

Again, defining

$$g_{20} = G(x_0, t) = At^{\gamma_1(x_0)} \quad (5.24)$$

at some initial higher value $x = x_0$, Eq.(5.21) can be expressed as

$$G(x, t) = g_{20} t^{\gamma_1(x) - \gamma_1(x_0)}. \quad (5.25)$$

Eq.(5.25) is the solution of the linear DGLAP equation at LO for gluon distribution at small- x with the ansatz of Eq.(5.5) and it describes the small- x behavior of

linear gluon density for a particular value of Q^2 by choosing an appropriate input distribution g_{20} from the initial boundary condition.

The effect of shadowing corrections to the gluon distribution function can be examined considering the solutions of the DGLAP and GLR-MQ equations respectively. To do this we calculate the ratio R_G of the predicted values of gluon distribution function obtained from the solution of nonlinear GLR-MQ equation given by Eq. (5.17) to that obtained using the linear DGLAP equation given by Eq.(5.25)

$$R_G = \frac{G^{GLR-MQ}(x, t)}{G^{DGLAP}(x, t)}, \quad (5.26)$$

as a function of variable x for different values of Q^2 . By evaluating this ratio we have observed a taming behavior of gluon distribution in the HERA kinematic region ($3 \leq \ln(1/x) \leq 12$) due to shadowing corrections to the linear evolution. Thus employing the expression (5.26) we can interpret the influence of nonlinear or shadowing corrections as a consequence of gluon recombinations on the behavior of gluon distribution at small- x . It also assists us to understand whether Froissart bound can be restored at small- x . We have explored the phenomenological aspect of Eq.(5.26) in section 3.

5.2.4 Compatibility of Regge like solutions of gluon density with the DLA solution

The DGLAP evolution equation predicts that the gluon distribution function rises steeply as a power of x toward small- x which is observed at HERA too. This is in accordance with the Double Logarithmic Approximation (DLA) at small- x and large photon virtualities Q^2 . The DLA accounts for only the leading double logarithmic contributions ($\alpha_s \ln(Q^2/Q_0^2) \ln(1/x)$) to multiparton cross sections. In DLA it is considered that $\frac{\alpha_s}{\pi} \ll 1$, $\frac{\alpha_s}{\pi} \ln Q^2 \ll 1$, $\frac{\alpha_s}{\pi} \ln^2 Q^2 \sim 1$ [38]. DLA analysis manifests the structure of intrajet parton cascades and as a matter of fact, the DLA predictions provide an assumption for the parton picture. The parton cascade is an excellent replica in consideration of DLA ladder diagrams. The DLA is applicable to perturbative QCD evolution in the asymptotic regime characterized by $Q^2 \gg Q_0^2$ and $x \ll x_0$, $x_0 \leq 0.1$, [39]. The proton structure function data explored at HERA have been demonstrated to evolve in consonance with DLA as suggested in Ref. [30]. The DLA asymptotics of the structure function derived by the addition of diagrams

corresponding to $(\alpha_s \ln(Q^2/Q_0^2))^n$ and of those $(\alpha_s \ln(1/x))^n$ occur simultaneously and produce the solution of the DGLAP equation in the form $\sim \exp\left(\sqrt{\ln \frac{t}{t_0} \ln \frac{x_0}{x}}\right)$ [9]. The gluon distribution produced by the DLA DGLAP evolution naturally portrays the data in a satisfactory manner exclusively in a somewhat confined kinematic domain of small- x and large- Q^2 .

Any LO solution of DGLAP equation is presumed to be consistent with the DLA result. That being so, it is worthwhile to investigate the prospect of compatibility of our Regge type solution of DGLAP equation with the DLA one. Even though Regge behavior is not in agreement with the DLA in general, but, when x is small enough ($x < 0.7$) the Regge theory is assumed to be applicable, whatsoever the value of Q^2 [34, 35]. Accordingly the Regge type solution of DGLAP equation is expected to be valid. The conventional DLA formula [38] for gluon distribution function is

$$G^{DLA}(x, t) = G(x, t_0) \exp\left(2\sqrt{\frac{N_c}{\pi b} \ln\left(\frac{t}{t_0}\right) \ln\left(\frac{x_0}{x}\right)}\right), \quad (5.27)$$

with the function $b = \frac{11N_c - 2N_f}{12\pi}$. Here $N_c = 3$ is the number of color. Our solution of linear DGLAP equation given by Eq. (5.25) is in agreement with DLA formula of Eq. (5.27) as long as the following condition is satisfied,

$$\frac{\ln\left(\frac{G^{DLA}(x, t_0)}{G^{DGLAP}(x_0, t)}\right)}{(\gamma_1(x) - \gamma_1(x_0))t} + \frac{2\sqrt{\frac{12N_c}{11N_c - 2N_f} \ln\left(\frac{t}{t_0}\right) \ln\left(\frac{x_0}{x}\right)}}{(\gamma_1(x) - \gamma_1(x_0))t} = 1. \quad (5.28)$$

An analysis of the phenomenological aspects of Eq.(5.28) is presented in section 3 where we denote the l.h.s. of Eq.(5.28) as $P(x, Q^2)$.

5.3 Result and discussion

We solve the nonlinear GLR-MQ evolution equation by considering the Regge like behavior of gluon distribution function and examine the effects of adding the non-linear GLR-MQ corrections due to gluon recombination processes at small- x to the LO DGLAP evolution equations. We investigate the behavior of gluon distribution function at small- x and moderate Q^2 from the predicted solution of the GLR-MQ equation. The solutions suggested in Eqs.(5.15) and (5.17) are directly related to the initial conditions. Our predictions of x and Q^2 dependence of gluon distribution function $G(x, Q^2)$ are compared with those obtained by the global QCD

fits to the parton distribution functions, viz. GRV1998LO [40], GJR2008LO [41], MRST2001LO [42], MSTW2008LO [43], NNPDF [44], HERAPDF0.1 [45, 46] and CT10 [47, 48] parametrizations respectively. To evolve our solutions, we use the GRV1998LO input and MRST2001LO input for two different representations of our solutions.

Furthermore, we present a comparative analysis of our computed results with the results of the EHKQS [20] and BZ models [23]. In the EHKQS model the effects of the first nonlinear corrections to the DGLAP evolution equations are studied by using the recent HERA data for the structure function $F_2(x, Q^2)$ of the free proton and the parton distributions from CTEQ5L and CTEQ6L as a baseline [49]. The EHKQS model shows that the nonlinear corrections improve the agreement with the $F_2(x, Q^2)$ data in the region of $x \sim 3 \times 10^{-5}$ and $Q^2 \sim 1.5 \text{ GeV}^2$. On the other hand in BZ model using a Laplace-transform technique, the behavior of the gluon distribution is obtained by solving the GLR-MQ evolution equation with the nonlinear shadowing term incorporated.

Figure 5.1 represent our predictions of the gluon distribution function with the effect of nonlinear or shadowing corrections obtained from Eq.(5.15), plotted against Q^2 for four fixed values of x , viz. $x = 10^{-2}, 10^{-3}, 10^{-4}$ and 10^{-5} respectively. We compare our predictions with GRV1998LO, GJR2008LO, MRST1001LO and MSTW2008LO global parton analysis as well as with the EHKQS model. The input distribution is taken from the GRV1998LO. The red solid curve represents the effect of the shadowing correction of gluon distribution function predicted by using Eq.(5.15) for the hot spots with $R = 2 \text{ GeV}^{-1}$ whereas the results for $R = 5 \text{ GeV}^{-1}$ is shown by the blue solid line.

Similarly, in Figure 5.2 we plot our computed results of the gluon distribution function obtained from Eq.(5.15) vs. Q^2 , considering the MRST2001LO input gluon distribution, for $x = 10^{-2}, 10^{-3}, 10^{-4}$ and 10^{-5} respectively as before. Here also the red and blue solid lines represent our predictions of nonlinear gluon density for $R = 2 \text{ GeV}^{-1}$ and $R = 5 \text{ GeV}^{-1}$ respectively. We perform a comparison of our results with different parametrizations namely, HERAPDF0.1, CT10 and NNPDF.

Figure 5.3 represent the small- x behavior of the gluon distribution with the effect shadowing corrections to the gluon distribution function determined from Eq.(5.17)

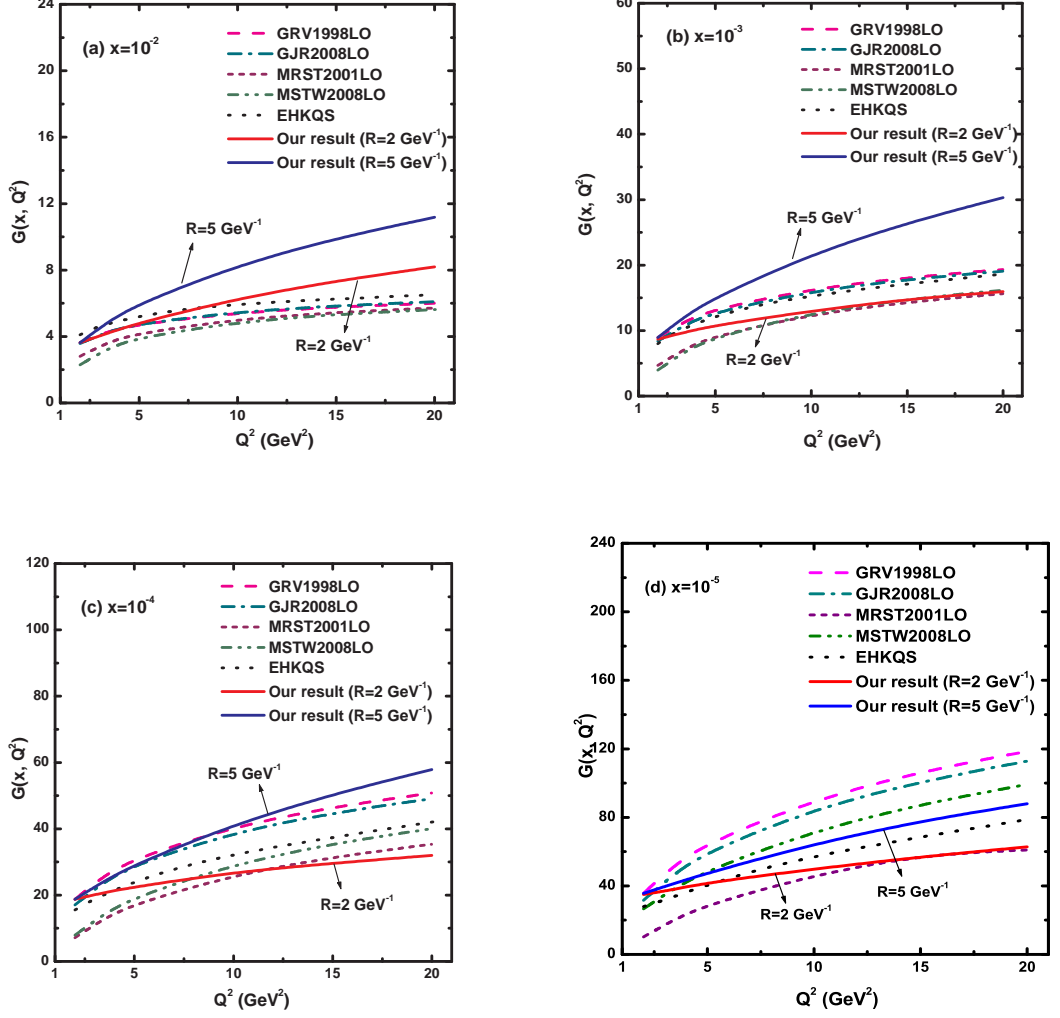


Figure 5.1: Q^2 dependence of gluon distribution with shadowing corrections obtained from Eq.(5.15) for four fixed values of x at $R = 2 \text{ GeV}^{-1}$ (red solid curves) and $R = 5 \text{ GeV}^{-1}$ (blue solid curves) respectively. Our predictions are compared with GRV1998LO (dash), GJR2008LO (dash-dot), MRST2001LO (short-dash) and MSTW2008LO (dash-dot-dot) parametrizations as well as with the EHKQS model (dot). The input gluon distribution is taken from GRV1998LO.

as a function of x for four fixed values of Q^2 , viz. $Q^2 = 5, 10, 15$ and 20 GeV^2 . Here the input gluon distribution is taken from GRV1998LO to evolve our solutions and our predictions of the small- x behaviour of nonlinear gluon density are compared with the global QCD analysis namely GRV1998LO, GJR2008LO, MRST2001LO, MSTW2008LO as well as with the H1 data. The red and blue solid lines represent our best fit results of nonlinear gluon density for $R = 2 \text{ GeV}^{-1}$ and $R = 5 \text{ GeV}^{-1}$ respectively.

On the other hand, our predictions of gluon distribution function with the shadowing corrections evaluated from Eq. (5.17) using the MRST2001LO input are plotted in Figure 5.4 as a function of x for four fixed Q^2 , viz. $Q^2 = 5, 10, 15$ and

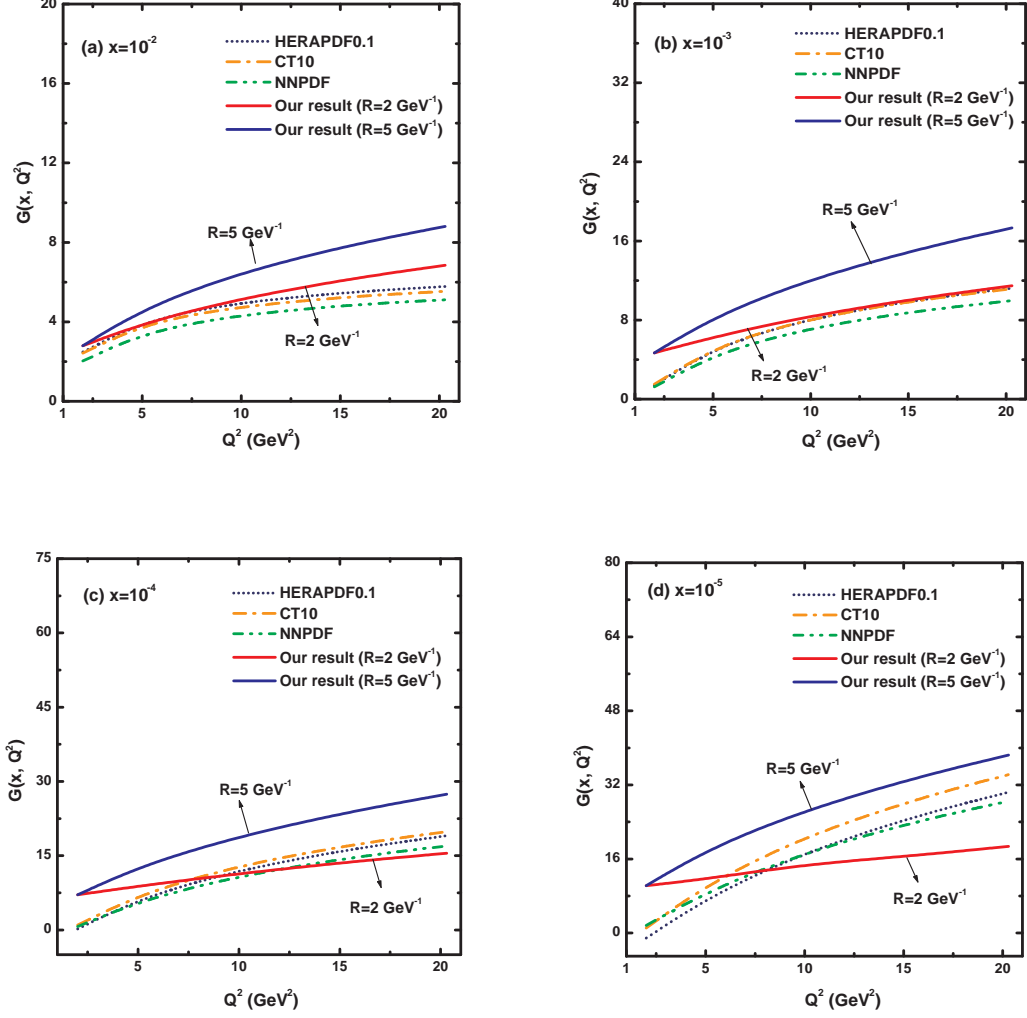


Figure 5.2: Q^2 dependence of gluon distribution function incorporating shadowing corrections computed from Eq.(5.15) for four fixed values of x at $R = 2 \text{ GeV}^{-1}$ (red solid curves) and $R = 5 \text{ GeV}^{-1}$ (blue solid curves) respectively. Our predictions are compared with HERAPDF0.1 (short-dot), CT10 (dash-dot) and NNPDF (dash-dot-dot) parametrizations. The input gluon distribution is taken from MRST2001LO.

20 GeV^2 as in the previous case. We make a comparison of our computed results of nonlinear gluon density with the HERAPDF0.1, CT10, NNPDF parametrizations as well as with the results of BZ model. Here too the computed results of the small- x behaviour of nonlinear gluon density corresponding to $R = 2 \text{ GeV}^{-1}$ and $R = 5 \text{ GeV}^{-1}$ are represented by the red and blue solid lines respectively.

From Figure 5.1 to Figure 5.4 we have observed that our results are in good agreement with different experimental data, global parametrizations and also with different models. The gluon distribution increases with increasing Q^2 and decreasing x , which complements the perturbative QCD fits at small- x , but this behaviour is tamed with respect to the nonlinear terms in GLR-MQ equation. It is very interesting to observe that our predictions for the x and Q^2 dependence of nonlinear gluon

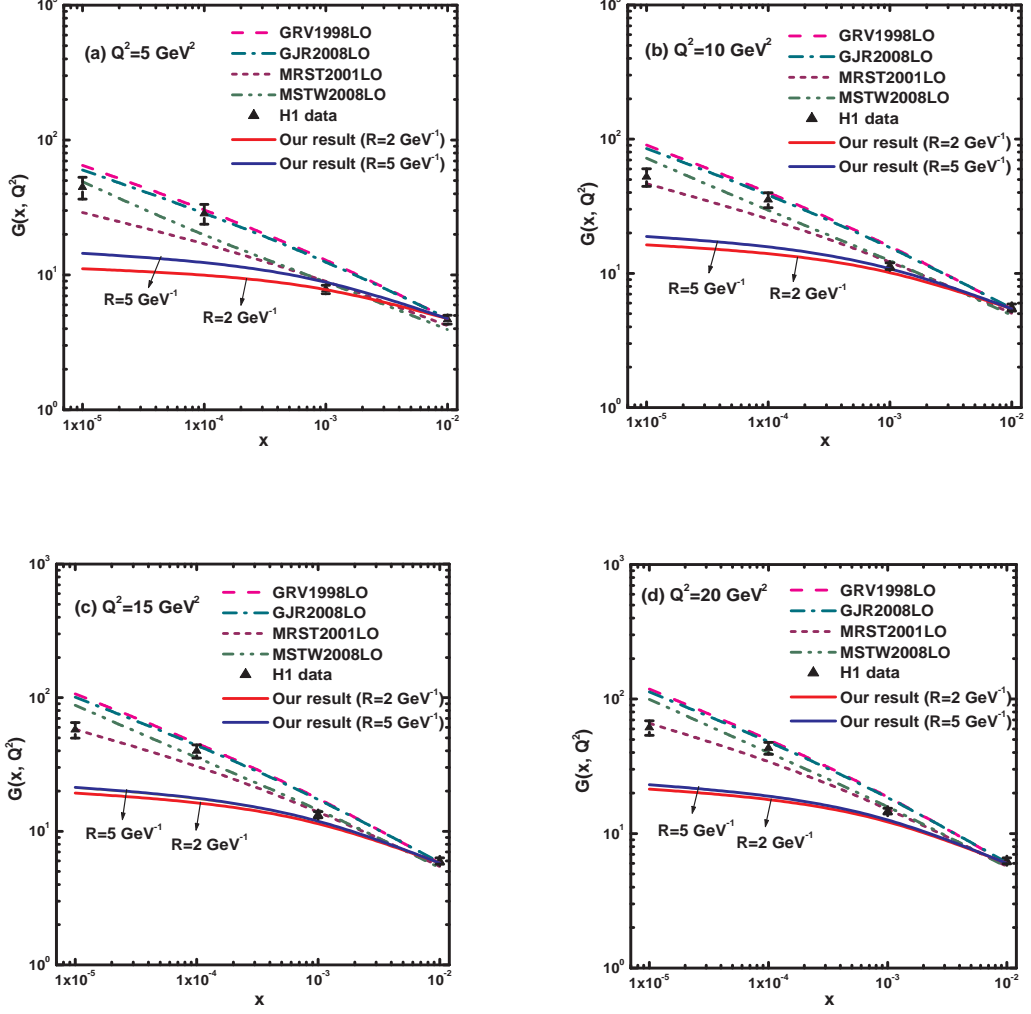


Figure 5.3: Small- x behaviour of gluon distribution with shadowing corrections obtained from Eq.(5.17) for four fixed values of Q^2 at $R = 2 \text{ GeV}^{-1}$ (red solid curves) and $R = 5 \text{ GeV}^{-1}$ (blue solid curves) respectively. Our results are compared with GRV1998LO (dash), GJR2008LO (dash-dot), MRST2001LO (short-dash), MSTW2008LO (dash-dot-dot) parametrizations as well as with H1 data (up-triangle). The input gluon distribution is taken from GRV1998LO.

density are in excellent agreement with the gluon density function obtained from HERAPDF0.1 and CT10 parametrizations. Moreover, we observe from Figure 5.2 that our results of the effect of shadowing corrections to the moderate- Q^2 behaviour of gluon distribution function are comparable with those obtained in a similar analysis by the EHKQS model. We further note that, our results follow the general trend of H1 data but they get saturated towards very small- x due to shadowing corrections. Similarly, we see that the shapes of the curves in Figure 5.4 representing the small- x behaviour of nonlinear gluon density are almost similar to the results of BZ model. Therefore we can say that the Regge type solution of the GLR-MQ equation for the nonlinear gluon distribution suggested in Eq.(5.11) can describe the available data in

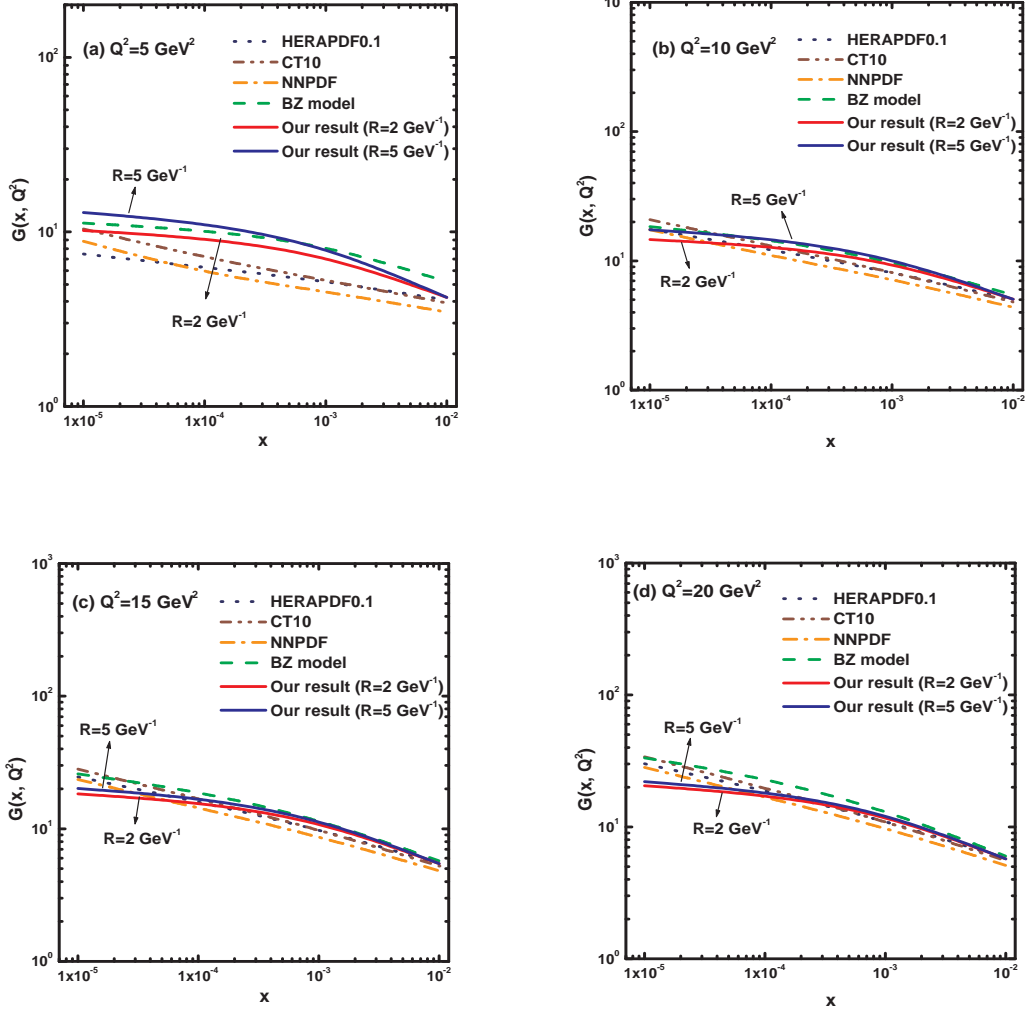


Figure 5.4: Small- x behaviour of gluon distribution considering shadowing corrections calculated from Eq.(5.17) for four fixed values of Q^2 at $R = 2 \text{ GeV}^{-1}$ (red solid curves) and $R = 5 \text{ GeV}^{-1}$ (blue solid curves) respectively. Our results are compared with HERAPDF0.1 (dot), CT10 (dash-dot-dot) and NNPDF (dash-dot) parametrizations and BZ model (dash). The input gluon distribution is taken from MRST2001LO.

a satisfactory manner. We perform our analysis in the kinematic region $1 \leq Q^2 \leq 30 \text{ GeV}^2$ and $10^{-5} \leq x \leq 10^{-2}$ and our solution of the nonlinear gluon density is found to be legitimate in this kinematic domain. The effect of shadowing corrections as a consequence of gluon recombination processes in our predictions is observed to be very high at the hot-spots with $R = 2 \text{ GeV}^{-1}$ when the gluons are centered within the proton, compared to at $R = 5 \text{ GeV}^{-1}$ when the gluons are disseminated throughout the entire proton.

Moreover, to examine the effects of nonlinear or shadowing corrections to the gluon distributions in our prediction, we have plotted the ratio R_G of the gluon distribution function obtained from the solution of nonlinear GLR-MQ equation for $R = 2 \text{ GeV}^{-1}$ to that obtained from the solution of linear DGLAP equation using Eq.(5.26)

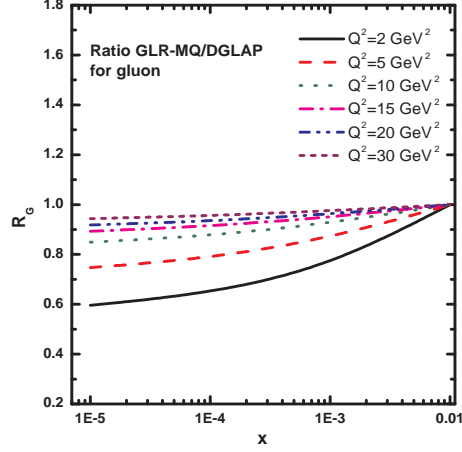


Figure 5.5: A comparison of the gluon distribution function in terms of R_G defined in Eq.(5.26). The comparison is shown for six different bins in $Q^2 = 2, 5, 10, 15, 20$ and 30 GeV^2 .

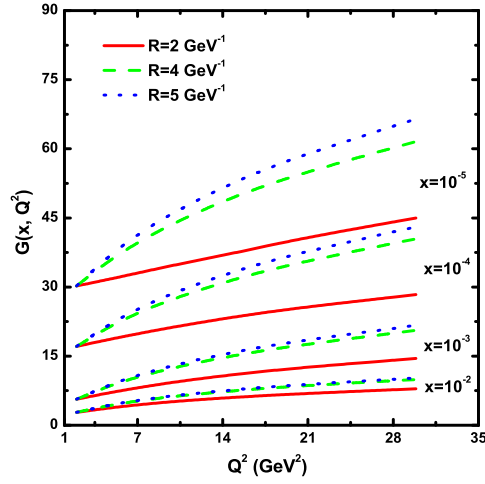


Figure 5.6: Sensitivity of the correlation radius R in our predictions for four values of x .

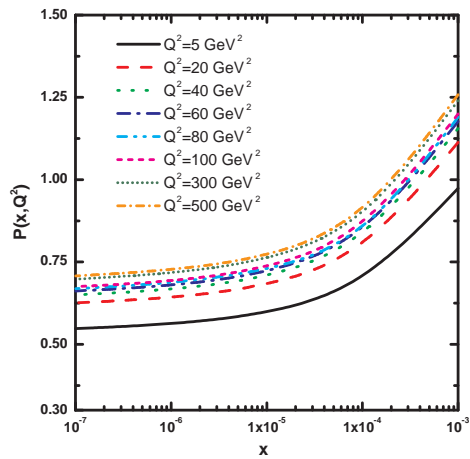


Figure 5.7: Compatibility of our LO solution of DGLAP equation with the DLA one using Eq.(5.28).

in Figure 5.5. This comparison helps us to estimate the shadowing corrections for the gluon distribution function. We plot the ratio R_G for gluon distribution as a function of the variable x for six representative values $Q^2 = 2, 5, 10, 15, 20$ and 30 GeV^2 respectively. We observe that as x grows smaller the GLR-MQ/DGLAP ratios decrease which implies that the effect of nonlinearity increases towards small- x due to gluon recombination. The fall of the ratio at small- x ($x < 10^{-2}$) is a consequence of the gluon recombination or shadowing corrections. Results also clearly indicates that towards smaller values of Q^2 the value of the ratio between nonlinear gluon density and linear gluon density also goes smaller. In other words, gluon recombination plays an important role in the region of small- x and Q^2 whereas, with the evolution to large- Q^2 ($Q^2 > 30 \text{ GeV}^2$) and large- x ($x \geq 10^{-2}$), gluon recombinations play less of a role, and as a consequence the nonlinear effects have a very little impact.

We have further investigated the effect of nonlinearity in our results by performing an analysis to check the sensitivity of the correlation radius R between two interacting gluons. For this analysis our computed values of $G(x, Q^2)$ from Eq. (5.15) for $R = 2, 4$ and 5 GeV^{-1} respectively are plotted against Q^2 in Figure 5.6 for four fixed values of x , $x = 10^{-2}, 10^{-3}, 10^{-4}$ and 10^{-5} . For this analysis we take the input distribution from MRST2001LO global parametrization for a given value of Q_0^2 . The gluon distribution function is observed to be more tamed at $R = 2 \text{ GeV}^{-1}$, where gluons are supposed to be condensed in the hot-spots within the proton, compared to at $R = 4 \text{ GeV}^{-1}$ and $R = 5 \text{ GeV}^{-1}$ where gluons are almost scattered over the entire proton. Moreover, we note that the differences between the data as we approach from $R = 2 \text{ GeV}^{-1}$ to $R = 5 \text{ GeV}^{-1}$ increase with decreasing x as anticipated.

Figure 5.7 represents the plot of $P(x, Q^2)$ vs. x for different values of Q^2 , where $P(x, Q^2)$ represents the l.h.s of Eq.(5.28) which represents the condition of compatibility of the Regge like solution of DGLAP equation to the DLA one. This figure illustrates that our Regge type solution of linear DGLAP equation given by Eq.(5.23) is comparable with the DLA result of Eq.(5.27) in a finite domain of x and Q^2 as long as the constraint given by Eq.(5.28) is fulfilled. It is obvious from the figure that for each value of Q^2 , there is a corresponding value of x for which the l.h.s and r.h.s. of Eq.(5.28) are identical and the value of x , where this happens, switches to lower limit as Q^2 increases. We observe that for the Q^2 values $5 \leq Q^2 \leq 500 \text{ GeV}^2$,

considered in our analysis, the condition of compatibility is satisfied in the region of x between 10^{-4} and 10^{-3} . Accordingly the Regge like solution of the linear DGLAP equation in LO is expected to be applicable in the region of $10^{-4} \leq x \leq 10^{-3}$ and high- Q^2 if it is appealed to be consistent with the DLA one.

5.4 Summary

In summary, the behavior of gluon distributions in the region of small- x and moderate- Q^2 are semi-analytically predicted by solving the nonlinear GLR-MQ equation in leading twist approximation incorporating the well known Regge ansatz. We make a deliberate attempt to explore the effect of nonlinear or shadowing corrections arises due to the gluon recombination processes on the behavior of gluon distribution at small- x and moderate- Q^2 . We observe that the gluon distribution function increases with increasing Q^2 and decreasing x , but with the inclusion of the nonlinear terms, this behaviour of gluon density is slowed down relative to DGLAP gluon distribution. We investigate how the inclusion of nonlinear effects changes the behavior of gluon density and it is interesting to observe that although the gluon distribution increases with increasing Q^2 and decreasing x as usual, which is in agreement with the perturbative QCD fits at small- x , however the gluon recombination processes tame the rapid growth of gluon densities towards small- x . This suggests that the gluon distributions unitarize leading to the restoration of Froissart bound in the small- x region where density of gluons becomes very high. For the gluon distribution the nonlinear effects are found to play an increasingly important role at $x \leq 10^{-3}$. The nonlinearities, however, vanish rapidly at larger values of x . Furthermore, our results manifest that the nonlinearity increases with decreasing value of correlation radius R as expected which is very fascinating.

Our results indicates that the nonlinear effects or shadowing corrections, emerged as a consequence of recombination of two gluon ladders, play a significant role on QCD evolution for gluon distribution in the kinematic region of small- x and moderate- Q^2 . Accordingly the suggested solution of the GLR-MQ equation for gluon distribution function is anticipated to be legitimate only in the vicinity of saturation i.e. in the kinematic region $1 \leq Q^2 \leq 30 \text{ GeV}^2$ and $10^{-5} \leq x \leq 10^{-2}$. Our phenomenological analysis also supports this as the obtained results of nonlinear gluon density using

the Regge ansatz are in accordance with different parametrization as well as models.

Finally, we derive the condition of compatibility of the LO solution of linear DGLAP equation for gluon, obtained by employing the Regge ansatz, with the DLA solution in a finite range of the variables x and Q^2 . From our phenomenological analysis we understand that in the Q^2 region $5 \leq Q^2 \leq 500 \text{ GeV}^2$, considered in our study, the condition of compatibility is satisfied in the region of x between 10^{-4} and 10^{-3} . Accordingly we can expect the Regge type solution of the linear DGLAP equation in LO to be applicable in the region of $10^{-4} \leq x \leq 10^{-3}$ and high- Q^2 if we demand it to be consistent with the DLA one.

Bibliography

- [1] Stasto, A. M., Golec-Biernat, K. J. and Kwiecinski, J. Geometric scaling for the total γ^*p cross section in the low x region, *Phys. Rev. Lett.* **86**(4), 596—599, 2001.
- [2] Albacete, J. L., Marquet, C. Azimuthal correlations of forward dihadrons in d+Au collisions at RHIC in the color glass condensate, *Phys. Rev. Lett.* **105**(16), 162301, 2010.
- [3] Dumitru, A. et al., The ridge in proton-proton collisions at the LHC, *Phys. Lett. B* **697**(1), 21—25, 2011.
- [4] Dokshitzer, Y. L. Calculation of structure functions of deep-inelastic scattering and e^+e^- annihilation by perturbation theory in quantum chromodynamics, *Sov. Phys. JETP* **46**(4), 641—652, 1977.
- [5] Altarelli, G., Parisi, G. Asymptotic freedom in parton language, *Nucl. Phys. B* **126**(2), 298—318, 1977.
- [6] Gribov, V. N., Lipatov, L. N. Deep inelastic ep scattering in perturbation theory, *Sov. J. Nucl. Phys.* **15**(4), 438—450, 1972.
- [7] Froissart, M. Asymptotic behavior and subtractions in the Mandelstam representation, *Phys. Rev.* **123**(3), 1053—1057, 1961.
- [8] Martin, A. Unitarity and high-energy behavior of scattering amplitudes, *Phys. Rev.* **129**(3), 1432—1436, 1963.
- [9] Gribov, L. N., Levin, E. M. and Ryskin, M. G. Semihard processes in QCD, *Phys. Rep.* **100**(1-2), 1—150, 1983.

- [10] Mueller, A. H., Qiu, J. Gluon Recombination and Shadowing at Small Values of x , *Nucl. Phys. B* **268**(2), 427—452, 1986.
- [11] Mueller, A. H. Small- x behavior and parton saturation: A QCD model, *Nucl. Phys. B* **335**(1), 115—137, 1990.
- [12] Abramovsky, V. A., Gribov, V. N., Kancheli, O. V. Character of inclusive spectra and fluctuations produced in inelastic processes by multi-Pomeron exchange, *Sov.J.Nucl.Phys.* **18**, 308—317, 1974.
- [13] Collins J. C., Kwiecinski, J. Shadowing in gluon distributions in the small- x region, *Nucl. Phys. B* **335**(1), 89—100, 1990.
- [14] Ayala, A. L., Gay Ducati, M. B. and Levin, E. M. QCD evolution of the gluon density in a nucleus, *Nucl. Phys. B* **493**(12), 305—353, 1997.
- [15] Ayala, A. L., Gay Ducati, M. B. and Levin, E. M. Parton densities in a nucleon, *Nucl. Phys. B* **511**(12), 355—395, 1998.
- [16] Bartels, J., Levin, E. Solutions to the Gribov-Levin-Ryskin equation in the nonperturbative region, *Nucl. Phys. B* **38**(3), 617—637, 1992.
- [17] Levin E., Tuchin, K. Solution to the evolution equation for high parton density QCD, *Nucl. Phys. B* **573**(3), 833—852, 2000.
- [18] Prytz, K. Signals of gluon recombination in deep inelastic scattering, *Eur. Phys. J. C* **22**(2), 317—321, 2001.
- [19] Bartels, J., Blumlein J. and Shuler, G. A Numerical study of the small x behavior of deep inelastic structure functions in QCD, *Z. Phys. C* **50**(1), 91—102, 1991.
- [20] Eskola, K. J. et al., Nonlinear corrections to the DGLAP equations in view of the HERA data, *Nucl. Phys. B* **660**(1-2), 211—224, 2003.
- [21] Watt, G., Martin, A. D. and Ryskin, M. G. Effect of absorptive corrections on inclusive parton distributions, *Phys. Lett. B* **627**(1-4), 97—104, 2005.

- [22] Rezaei, B., Boroun, G. R. Analytical approach for the approximate solution of the longitudinal structure function with respect to the GLR-MQ equation at small x , *Phys. Lett. B* **692**(4), 247––249, 2010.
- [23] Boroun, G. R., Zarrin, S. An approximate approach to the nonlinear DGLAP evaluation equation, *Eur. Phys. J. Plus* **128**(10), 119, 2013.
- [24] Laenen, E., Levin, E. A new evolution equation, *Nucl. Phys. B* **451**(1-2), 207––230, 1995.
- [25] Laenen, E., Levin, E. Parton densities at high energy, *Annu. Rev. Nucl. Part. Sci.* **44**, 199––246, 1994.
- [26] Levin, E. M., Ryskin, M. G. Low- x structure function and saturation of the parton density, *Nucl. Phys. B (Proc. Suppl.)* **18**(3), 92––124, 1991.
- [27] Abbott, L. F., Atwood, W. B. and Michael Barnett, R. Quantum-chromodynamic analysis of eN deep-inelastic scattering data, *Phys. Rev. D* **22**(3), 582––594, 1980.
- [28] Collins, P. D., *An Introduction to Regge Theory and High-Energy Physics*, Cambridge University Press, Cambridge, 1997.
- [29] Donnachie, A., Landshoff, P. V. Total cross sections, *Phys. Lett. B* **296**(1-2), 227–– 232, 1992.
- [30] Ball, R. D., Forte, S. Double asymptotic scaling at HERA, *Phys. Lett. B* **335**(1), 77––86, 1994
- [31] Kotikov, A. V. Small x Behaviour of parton distributions in proton, *Mod. Phys. Lett. A* **11**(2), 103, 1996.
- [32] Kwiecinski, J. Theoretical issues of small x physics, *J. Phys. G: Nucl. Part. Phys.* **22**(6), 685––702, 1996.
- [33] Donnachie, A., Landshoff, P. V. Small x : two pomerons!, *Phys. Lett. B* **437**(3-4), 408––416, 1998.

- [34] Bartels, J. et al., The dipole picture and saturation in soft processes, *Phys. Lett. B* **556**(3-4), 114––122, 2003.
- [35] Martin, A. D., Ryskin, M. G. and Watt, G. Simultaneous QCD analysis of diffractive and inclusive deep-inelastic scattering data, *Phys. Rev. D* **70**(9), 091502, 2004.
- [36] Badelek, B. Spin Dependent Structure Function $g_1(x, Q^2)$ at Low x and Low Q^2 , *Acta Phys. Polon. B* **34**(6), 2943––2962, 2003.
- [37] Soffer, J., Teryaev, O. V. Neutron spin-dependent structure function, Bjorken sum rule, and first evidence for singlet contribution at low x , *Phys. Rev. D* **56**(3), 1549, 1997.
- [38] Dokshitzer, Y. L., Khoze, V. A., Mueller, A. H. and Troyan, S. I. *Basics of Perturbative QCD*, Editions Frontieres, Fong and Sons Printers Pte. Ltd, Singapore, 1991.
- [39] De Rujula, A. et al., Possible non-Regge behavior of electroproduction structure functions, *Phys. Rev. D* **10**(5), 1649, 1974.
- [40] Gluck, M., Reya, E. and Vogt, A. Dynamical parton distributions revisited, *Eur. Phys. J. C* **5**(461), 470, 1998.
- [41] Gluck, M., Jimenez-Delgado, P. and Reya, E. Dynamical parton distributions of the nucleon and very small- x physics, *Eur. Phys. J. C* **53**(3), 355––366, 2008.
- [42] Martin, A. D. et al., MRST2001: partons and α_s from precise deep inelastic scattering and Tevatron jet data, *Eur. Phys. J. C* **23**(1), 73––87, 2002.
- [43] Martin, A. D. et al., Parton distributions for the LHC, *Eur. Phys. J. C* **63**(2), 189––285, 2009.
- [44] Forte, S. et al., Neural network parametrization of deep inelastic structure functions, *JHEP* **2002**(JHEP05), 062, 2002.
- [45] Adloff, C. et al., Measurement and QCD analysis of neutral and charged current cross sections at HERA, *Eur. Phys. J. C* **30**(1), 1––32, 2003.

- [46] S. Chekanov et al., An NLO QCD analysis of inclusive cross-section and jet-production data from the ZEUS experiment, *Eur. Phys. J. C* **42**(1), 1–16, 2005.
- [47] Guzzi, M. et al., CT10 parton distributions and other developments in the global QCD analysis, *arXiv:1101.0561v1*.
- [48] Lai, H. L. et al., New parton distributions for collider physics, *Phys. Rev. D* **82**(7), 074024, 2010.
- [49] Pumplin, J. et al., New generation of parton distributions with uncertainties from global QCD analysis, *JHEP* **2002**(07), 012, 2002.